Biological Probes Hot Paper

How to cite: *Angew. Chem. Int. Ed.* **2021**, *60*, 11143–11147
International Edition: doi.org/10.1002/anie.202016880
German Edition: doi.org/10.1002/ange.202016880

A Genetically Encoded Two-Dimensional Infrared Probe for Enzyme Active-Site Dynamics

Li Wang[+], Jia Zhang[+], Ming-Jie Han[+], Lu Zhang[+], Chao Chen[+], Aiping Huang[+], Ruipei Xie, Guosheng Wang, Jiangrui Zhu, Yuchuan Wang, Xiaohong Liu, Wei Zhuang,* Yunliang Li,* and Jiangyun Wang**

Abstract: *While two-dimensional infrared (2D-IR) spectroscopy is uniquely suitable for monitoring femtosecond (fs) to picosecond (ps) water dynamics around static protein structures, its utility for probing enzyme active-site dynamics is limited due to the lack of site-specific 2D-IR probes. We demonstrate the genetic incorporation of a novel 2D-IR probe, m-azido-L-tyrosine (N3Y) in the active-site of DddK, an iron-dependent enzyme that catalyzes the conversion of dimethylsulfoniopropionate to dimethylsulphide. Our results show that both the oxidation of active-site iron to Fe^{III}, and the addition of denaturation reagents, result in significant decrease in enzyme activity and active-site water motion confinement. As tyrosine residues play important roles, including as general acids and bases, and electron transfer agents in many key enzymes, the genetically encoded 2D-IR probe N3Y should be broadly applicable to investigate how the enzyme active-site motions at the fs–ps time scale direct reaction pathways to facilitating specific chemical reactions.*

Enzymes move on a large variety of time scales from femtoseconds to seconds.[1] While much is known about how slow motions (i.e., milliseconds to seconds) impact substrate binding and product release, little is known about how fast motions occurring on femtosecond (fs) to picosecond (ps) time scale influence enzyme activity.[1b,c,2] It has been suggested that the enzyme nanosecond time scale fast motion are capable of directing large-scale slow motions and reactions along the correct pathway, facilitating specific chemical reactions.[1a,3] However, many aspects of this structure–activity correlation, especially at fs–ps time scale, remain unexplored. Since chemical reaction transition states occur in fs timescale,[1c] the development of protein labelling and spectroscopic tools to facilitate the observation of fs–ps timescale dynamics in enzymes is especially important. Tremendous effort has been dedicated to developing experimental tools[4] for detecting these fast fluctuations at the enzyme active-site. Among these methods, two-dimensional infrared (2D-IR) spectroscopy has an intrinsic fast time resolution[1c,5] uniquely suitable for monitoring fs–ps water and ion dynamics, around static protein structures.[6]

Indeed, recent advancements in protein site-specific IR probe greatly improved the spatial resolution of time-resolved infrared technique, and pushed it towards a highly informative tool for the protein dynamic studies. For example, genetically encoded unnatural amino acids, such as *p*-azido-L-phenylalanine (N3F)[7] and *p*-cyano-L-phenylalanine (CNF)[8] (Figure 1 a), have been used to track local electric field, characterize protein folding kinetics and protein/protein interactions.[2a,c] However, since phenylalanine sidechains are mostly buried inside protein hydrophobic core, and usually do not directly participate in enzyme catalysts, these

[*] Dr. M.-J. Han,[+] Dr. C. Chen,[+] Dr. A. Huang[+]
Tianjin Institute of Industrial Biotechnology
Chinese Academy of Sciences
West 7th Avenue, Tianjin Airport Economic Area
Tianjin 300308 (China)

Dr. L. Wang[+]
School of Life Sciences, University of Chinese Academy of Sciences
Yuquan Road, Shijingshan District, Beijing 100049 (China)

J. Zhang,[+] R. Xie, G. Wang, J. Zhu, Prof. Y. Li
Beijing National Laboratory for Condensed Matter Physics and Laboratory of Soft Matter Physics, Institute of Physics
Chinese Academy of Sciences
Beijing 100190 (China)
E-mail: yunliangli@iphy.ac.cn

L. Zhang,[+] Prof. W. Zhuang
State Key Laboratory of Structural Chemistry, Fujian Institute of Research on the Structure of Matter, Chinese Academy of Sciences
Fuzhou 350002 (China)
E-mail: wzhuang@fjirsm.ac.cn

Dr. L. Wang,[+] Dr. X. Liu, Prof. J. Wang
Institute of Biophysics, Chinese Academy of Sciences
Datun Road, Chaoyang District, Beijing 100101 (China)
E-mail: liuxh@moon.ibp.ac.cn
jwang@ibp.ac.cn

Dr. M.-J. Han,[+] Dr. Y. Wang, Prof. J. Wang
Shenzhen Institute of Transfusion Medicine, Shenzhen Blood Center
Futian District, Shenzhen 518052 (China)

Prof. J. Wang
School of Life Sciences, University of Chinese Academy of Sciences
Yuquan Road, Shijingshan District, Beijing 100049 (China)

J. Zhang,[+] R. Xie, J. Zhu, Prof. Y. Li
School of Physical Sciences
University of Chinese Academy of Sciences
Beijing 100049 (China)

Prof. Y. Li
Songshan Lake Materials Laboratory
Dongguan, Guangdong 523808 (China)

Prof. W. Zhuang
Institute of urban environment, Chinese Academy of Sciences
Xiamen, Fujian 361021 (China)

[+] These authors contributed equally to this work.

Supporting information and the ORCID identification number(s) for the author(s) of this article can be found under: https://doi.org/10.1002/anie.202016880.

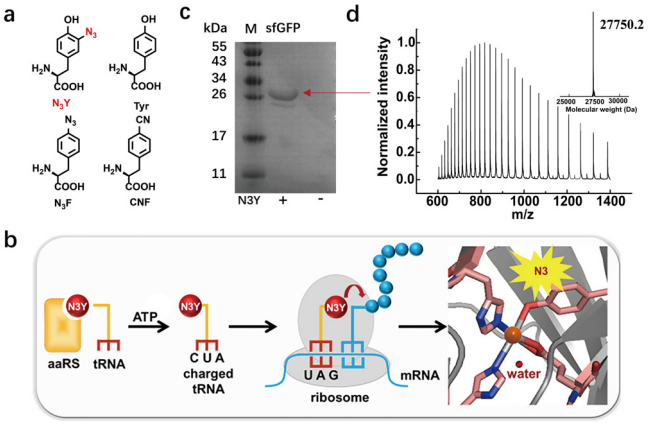

Figure 1. Site-specific incorporation of N3Y into a protein. a) Chemical structures of N3Y, Tyr, N3F, and CNF. b) The flow chart of incorporation of N3Y into protein. c) SDS-PAGE analysis of the purified sfGFP-66N3Y. d) ESI-MS spectrum of the sfGFP-66N3Y. The expected molecular weight is 27 750 Da; experimental molecular weight is 27 750.27 Da.

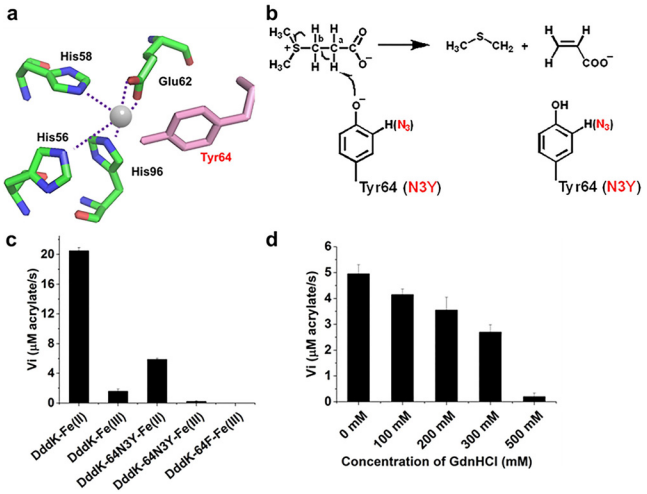

Figure 2. The catalytic mechanism by which DddK cleaves DMSP. a) The structure of the active-site in DddK (PDB: 5tg0). b) Mechanism of DddK, which catalyzes DMSP cleavage. Tyr64 residue acts as a base for proton abstraction from the DMSP substrate. c) The catalytic activity of DddK mutants, coordinating with Fe^{II} or Fe^{III}. d) The catalytic activity of DddK-64N3Y-Fe^{II} in the presence of various concentrations of GdnHCl.

genetically encoded phenylalanine analogues have limited utility for probing enzyme active-site dynamics.

Tyrosine residues are ubiquitous in the actives-site of many enzymes[9] 1) as a nucleophile, 2) as a general base for proton abstraction, 3) as a general acid for leaving group protonation, 4) they can participate in redox reactions, 5) form cation–pi interactions, and 6) coordinate with metal ions.[1b] Tyrosine residues therefore play pivotal roles in nucleic acid biosynthesis, DNA repair, dioxygen reduction by cytochrome oxidase, water oxidation by PSII, and many other biological processes.[3e] However, no tyrosine analogs have been site-specifically introduced into proteins, as 2D-IR probes.

In this work, we demonstrate the genetic incorporation of an 2D-IR probe (Figure 1b–d), *m*-azido-L-tyrosine (N3Y) into a metalloenzyme DddK. DddK is a metalloenzyme which converts one of the earth's most abundant organosulfur molecule dimethylsulfoniopropionate (DMSP) to dimethylsulphide (DMS, a central molecule in the marine sulfur cycle which is important in climate regulation)[10] and acrylate (Ddd: DMSP dependence DMS releasing). Residue Tyr64 at the active-site is proposed to play an important role[11] in metal binding, and catalytic activity (Figure 2a,b). The substitution of Tyr64 by N3Y, which added a small azido group in the ortho-position of the tyrosine sidechain, caused only small perturbation to the enzyme active-site, and the enzyme remains active (Figure 2c). Importantly, the large molar extinction coefficient of the azide stretching vibration in N3Y (about 1000 $M^{-1}cm^{-1}$) makes it an excellent sensor for protein dynamics.[2c,3b,10]

The unnatural amino acid N3Y was synthesized starting from *p*-aminophenylalanine (Supporting Information, Figures S1–S3), with an overall yield of 60%. To selectively incorporate N3Y at defined sites of proteins in *E. coli*, a mutant *Methanococcus jannaschii* tyrosyl amber suppressor tRNA ($MjRNA^{Tyr}_{CUA}$)/tyrosyl-tRNA synthetase (*Mj*TyrRS) pair was evolved that uniquely specified N3Y in response to the TAG codon.[12] An N3Y-specific TyrRS mutant termed N3YRS emerged after three rounds of positive selections and two rounds of negative selections, which grew with 120 μg mL^{-1} of chloramphenicol in the presence of 1 mM N3Y, but did not grow with 20 μg mL^{-1} of chloramphenicol in its absence. Sequencing of this clone revealed the following mutations: His70Ala, Asp158Ser, and Ile159Ser (Figure 1a,b). To further verify that the incorporation of N3Y into the target protein has high efficiency and fidelity, the amber stop codon TAG was substituted in the 66th position of superfolder green fluorescent protein (sfGFP). Protein expression and SDS-PAGE characterization results confirmed that the full-length sfGFP was expressed only in the presence of N3Y (Figure 1a), indicating that N3YRS was specifically active for N3Y but inactive for the natural amino acids. The yield for the sfYFP Tyr66-N3Y mutant of sfGFP was 20 mg L^{-1}. LC-MS analysis of sfGFP-66N3Y gave an observed average mass of 27 750.27 Da, in agreement with the calculated mass of sfGFP-66N3Y (27 750 Da, Figure 1b).

We then over-expressed DddK-64N3Y protein, by co-transforming pEVOL-N3YRS and pEt-DddK64TAG plasmids into BL21(DE3) *Escherichia coli* cells. In the presence of 1 mM N3Y, full-length DddK-64N3Y protein was overexpressed and obtained in 5 mg L^{-1} yield after His-tag affinity column purification. The SDS-PAGE and mass spectrometric analysis showed the successful incorporation of N3Y at the desired position in DddK with approximately 100% efficiency after purification (Figure S4). The Fe^{III} bound holoenzyme was obtained through the addition of ferric sulfate to apo DddK, and the Fe^{II} bound DddK was obtained through the reduction of the ferric state by the addition of 10 mM sodium dithionite (Figure S5). The catalytic activity of DddK enzymes was measured through an LC-MS assay.[11] Interestingly, the catalytic activity of Fe^{III} bound DddK (DddK-Fe^{III}) decreases for about ten folds in comparison to Fe^{II} bound DddK (DddK-Fe^{II}) (Figure S2b). When Tyr64 was mutated to phenylalanine, the catalytic activity of DddK was lost

completely (Figure 2c), which confirmed the key role of Tyr64 residue as a base for proton abstraction from the substrate[11] (Figure 2a). The substitution of N3Y to Tyr64 led to a threefold drop in DddK catalytic activity (Figure 2c). This might be attributed in part to the electron-withdrawing property of the azido functional group, decreasing N3Y's ability to extract a proton from DSMP substrate in comparison to tyrosine.

We measured the one-dimensional Fourier-transform infrared (1D-FTIR) spectra for both Fe^{III} and Fe^{II} bound states of DddK mutants (Figure 3a). The normalized and background subtracted 1D-FTIR spectra of DddK mutants have two well-separated peaks locate at 2119.2 cm^{-1}/2085.0 cm^{-1} for DddK-64N3Y-Fe^{III} and 2120.7 cm^{-1}/2087.9 cm^{-1} for DddK-64N3Y-Fe^{II}, respectively. The peak with higher intensity corresponds to the azido asymmetric stretch vibration, while the lower intensity peak originates from the Fermi Resonance.[1c,13] The wider FWHM (full width at half maxima) of azido asymmetric stretch band in DddK-64N3Y-Fe^{II} than in DddK-64N3Y-Fe^{III} suggests a more inhomogeneous distribution of local environments in DddK-64N3Y-Fe^{II} than DddK-64N3Y-Fe^{III}.

The 2D-IR spectra of the DddK mutants were then measured at various waiting times. Figure 3b displays the 2D-IR plots at $T = 0$ fs, 500 fs and 900 fs, respectively. The positive (red) peaks in each spectrum correspond to ground state bleach and stimulated emission, while the negative (blue) peaks represent the excited-state absorption. At $T =$ 0 fs, the detected frequency nicely correlates with the excited frequency, giving rise to the elongated elliptic shape along the diagonal line in the 2D plot. As waiting time increases, due to the losses of frequency-frequency correlation caused by the conformational fluctuation, the shape of 2D-IR spectra becomes more circular.

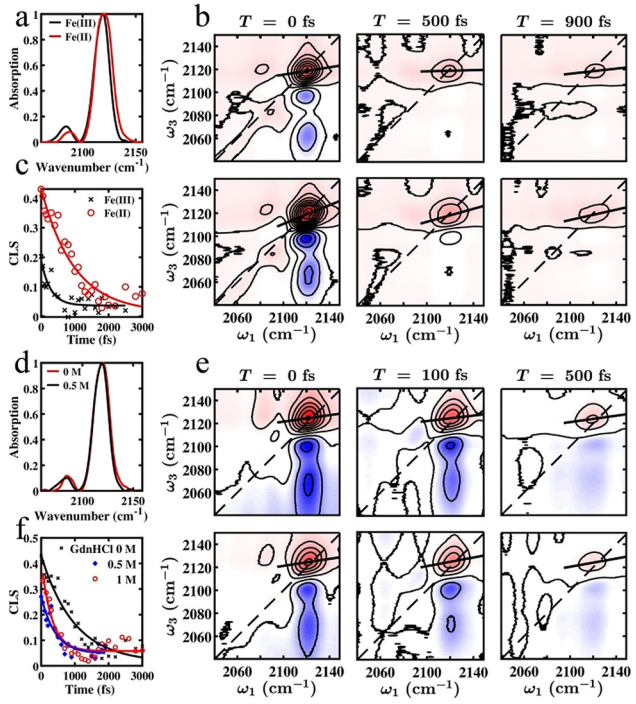

Figure 3. a) Normalized FTIR spectra of DddK-64N3Y-Fe^{III} and DddK-64N3Y-Fe^{II}. b) 2D-IR spectra of DddK-64N3Y-Fe^{III} (top) and DddK-64N3Y-Fe^{II} (bottom) with the waiting time increasing from 0 fs to 900 fs. c) FFCF dynamics of the azido asymmetric stretch vibration of DddK-64N3Y-Fe^{III} and DddK-64N3Y-Fe^{II}. d) Normalized FTIR spectra of DddK-64N3Y-Fe^{II} in the absence or presence of 0.5 M GdnHCl. e) 2D-IR spectra of DddK-64N3Y-Fe^{II} with the waiting time increasing from 0 fs to 500 fs, in the presence of 0.5 mM (top) and 1 M GdnHCl (bottom). f) FFCF dynamics of the azido asymmetric stretch vibration of DddK-64N3Y-Fe^{II} in the presence of various concentrations of GdnHCl.

To quantitatively extract and analyze the molecular dynamics information near the enzyme active site around the 64N3Y azide group, the frequency-frequency correlation function (FFCF) was analyzed for both DddK-64N3Y-Fe^{III} and DddK-64N3Y-Fe^{II} by fitting the centerline slope (CLS; Figure 3c).[1c,14] FFCF gives the insight on the molecular details, such as the time scales, of the processes involved in spectral diffusion within the inspected frequency windows.[15] Previous studies revealed that the decay time constant of FFCF for water hydrogen bond fluctuations in the bulk water is $\approx$170 fs, while those in the confined water vary from several hundred femtoseconds to a few picoseconds depending on the confinements. For the protein conformational fluctuations, on the other hand, the related FFCF decay with the time constants ranging from several picosecond to several nanosecond or even longer.[16] The fastest decay time constant of FFCF for the DddK-64N3Y-Fe^{III} is 150 ± 50 fs. This is consistent with the time constant of unconfined water dynamics in the bulk and much faster than the reported timescales of protein conformational fluctuations. By contrast, the fastest time constant of FFCF for DddK-64N3Y-Fe^{II} signal has a much larger time constant of 1050 ± 220 fs, which is consistent with the more confined water motion[17] in comparison to that of the DddK-64N3Y-Fe^{III} complex. Since high frequency localized vibrations such as the azido asymmetric stretch tend to be sensitive to the processes happening near the azido group at the active site, and a recent structural and mutational analyses of DddK by Peng et al. indeed revealed the existence of water near the active site,[18] it is reasonable to deduce that the femtosecond FFCF decay time constants observed reflect the water dynamics at the active sites.

We then analyzed how guanidinium hydrochloride (GdnHCl), a well-known protein denaturing reagent,[19] modulates DddK enzyme activity and active-site dynamics. As Figure 2d shows, Dddk-64N3Y-Fe^{II} enzyme activity begins to decrease in the presence of low concentration GdnHCl, and is lost completely in the presence of 0.5 M GdnHCl. Under these conditions, no significant change in DddK intrinsic tryptophan fluorescence was observed (Figure S6), indicating that there is no significant change in the overall DddK structure. These observations are consistent with the results of previous studies that in the presence of a low concentration of denaturing reagents, the enzyme activity is lost before protein denaturation.[20]

The effect of GdnHCl on DddK-64N3Y-Fe^{II} active-site dynamics was then investigated by 1D and 2D-IR spectroscopy. Upon the addition of 0.5 M GdnHCl, the FTIR spectrum (Figure 3d) of DddK-64N3Y-Fe^{II} undergoes

a minor frequency shift, which suggests an insignificant variation of local electrostatic environment in the active-site. The CLS decay time constant of the 2D-IR spectra (Figure 3 f) of DddK-64N3Y-Fe^{II} is 1050 ± 220 fs in the absence of GdnHCl, consistent with confined water in DddK active-site. The CLS decay time constant decreases to 410 ± 104 fs in the presence of 0.5 M GdnHCl, and to 310 ± 50 fs in 1 M GdnHCl, respectively. Addition of GdnHCl therefore speeds up the decay of CLS, consistent with less confined water in DddK active-site.

To further understand the molecular mechanism of the observed variations in the FFCF relaxation, we carried out 200 ns molecular dynamics simulations for 1) solvated DddK-64N3Y-Fe^{II}, 2) solvated DddK-64N3Y-Fe^{III} as well as 3) DddK-64N3Y-Fe^{II} in the aqueous solution of 1 M GdnHCl (for details, see the Supporting Information, Figures S7–S9). For all the three systems, we then calculated the instantaneous frequency $\omega_{total}(t)$ of azido asymmetric stretch vibration for each of the 1 000 000 MD snapshots along the trajectory, using an ab initio map connecting the instantaneous azido frequency to the electric field imposed by the environment (for details, see the Supporting Information). The distributions and time correlation functions of $\omega_{total}(t)$ for all the three systems are presented in Figure 4 a,b. Due to the additive nature of the electric field, $\omega_{total}(t)$ can be decomposed into the contributions of protein electric field $\omega_{protein}(t)$ and water electric field $\omega_{water}(t)$. Their distributions and time correlation functions are presented in Figure 4 c–f.

Consistent with the observations in the 1D FTIR experiments (Figure 3), the distribution of $\omega_{total}(t)$ in DddK-64N3Y-Fe^{III} and DddK-64N3Y-Fe^{II}-1M GdnHCl are red-shifted with respect to that in DddK-64N3Y-Fe^{II}. And this shift is mainly caused by the protein contribution $\omega_{protein}(t)$ Consistent with the experimental results, the computed FFCF $\omega_{total}(t)$ for DddK-64N3Y-Fe^{II} decays slower than that of DddK-64N3Y-Fe^{III}. The addition of guanidine (DddK-64N3Y-Fe^{II}-1 M GdnHCl) accelerates the decay of FFCF. Furthermore, FFCFs of $\omega_{protein}(t)$ are nearly-identical in all the three systems, while the FFCFs of $\omega_{water}(t)$ are significantly different. Our simulation therefore supports the picture that the aforementioned changes of FFCF decay behavior in the experiments are indeed caused by the differences of water hydrogen bond dynamics in DddK active-site.

In summary, we have shown that the genetically encoded unnatural amino acid N3Y is an excellent 2D-IR probe for the investigation of enzyme active-site dynamics at the fs–ps timescale. Our 2D-IR measurements provide direct evidence that the redox state change of the central iron atom in DddK strongly influences the fs–ps timescale water dynamics, indicating that N3Y is an environmentally sensitive 2D-IR probe. The addition of a low concentration of denaturation reagent also strongly influences DddK active-site water dynamics, without causing overall protein structural change. In both cases, our results show that less confined water in the DddK active-site is correlated with a decrease in enzyme activity.

With the structural characterization and mutational analyses of DddK, Peng et al. found that a Tyr64 residue forms a hydrogen bond with an active site water molecule,

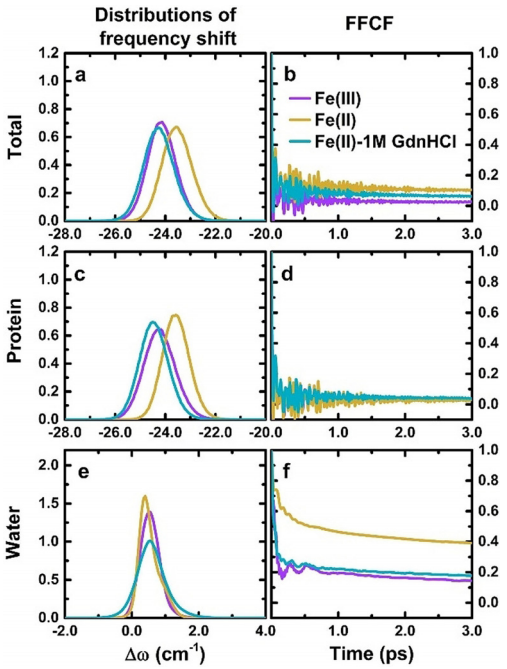

Figure 4. a) Distributions of the frequency shift induced by the complete system, c) only protein residues, and e) only the water molecules; calculated based on the molecular dynamics simulations. b) FFCF computed by including the complete system, d) only protein residues, and f) only water molecules; calculated based on the molecular dynamics simulations. Result key: DddK-64N3Y-Fe^{III} (purple), DddK-64N3Y-Fe^{II} (yellow), and DddK-64N3Y-Fe^{II}-1M GdnHCl (green).

with the distance of 2.6 Å.[18] Their work indicated that during the catalytic cycle of DddK, a water molecule activates Tyr64 for deprotonation, and therefore Tyr64 gain the ability to be a catalytic base. This work provides strong support on the connection between active site waters and DddK catalysis.[18]

Three decades ago, Chen-Lu Tsou made the first and important observation that the addition of a low concentration of protein denaturation reagents lead to the complete loss of enzyme activity, while the overall protein structure remained intact. Based on these observations, he put forth an important theory that the conformational flexibility of enzyme active sites is important in dictating enzyme activity.[20a] Our results provide new insight on how a low concentration of protein denaturation significantly decreases water confinement in an enzyme active-site, which might provide a mechanistic basis for why a low concentration of protein denaturation reagent is capable of abolishing enzyme activity without causing overall protein structural change. In future work, a large number of enzymes might be tested using the N3Y 2D-IR probe to verify this model. As 2D-IR is uniquely suited for characterizing protein dynamics in fs–ps time scale, and N3Y is an excellent environmental 2D-IR probe that can be used to replace tyrosine residues in an enzyme active-site while causing minimal perturbation to enzyme activity, our new method should be broadly applicable for studying tyrosine's diverse functions, and investigating how fs–ps time scale enzyme active-site dynamics influences enzyme selectivity and activity. In addition, we notice that two tyrosine residues (Tyr78 and Tyr82) are present in close

proximity to the potassium binding site of the K^+ ion channel structure (pdb code 1k4c).[21] The incorporation of N3Y in these sites may provide new insight into the K^+ ion channel mechanism and function.

Acknowledgements

We thank S. S. Zang and X.-H. L for help with NMR spectra determination, and X. Ding and Z. Xie for protein mass spectrometry measurement. We thank the "Strategic Priority Research Program" of the Chinese Academy of Sciences (XDB37040203), the National Key R&D Program of China (2016YFA0501502, 2019YFA0904101, 2018YFA0901602 and 2017YFA0503704), National Science Foundation of China (21837005, 91953202, 21890743, 21873101, 21961142014, 91953202, 22073111, 21573281, 21503268 to M.-J.H.), the FJIRSM&IUE Joint Research Fund (No. RHZX-2019-002), and the Sanming Project of Medicine in Shenzhen (No. SZSM201811092).

Conflict of interest

The authors declare no conflict of interest.

Keywords: azido-tyrosine · infrared spectroscopy · metalloenzymes · unnatural amino acid · water

[1] a) K. Henzler-Wildman, D. Kern, *Nature* **2007**, *450*, 964 – 972; b) R. Otten, R. A. P. Padua, H. A. Bunzel, V. Nguyen, W. Pitsawong, M. Patterson, S. Sui, S. L. Perry, A. E. Cohen, D. Hilvert, D. Kern, *Science* **2020**, *370*, 1442 – 1446; c) A. Ghosh, J. S. Ostrander, M. T. Zanni, *Chem. Rev.* **2017**, *117*, 10726 – 10759.

[2] a) S. D. Fried, S. G. Boxer, *Annu. Rev. Biochem.* **2017**, *86*, 387 – 415; b) J. Q. Ma, I. M. Pazos, W. K. Zhang, R. M. Culik, F. Gai, *Annu. Rev. Phys. Chem.* **2015**, *66*, 357 – 377; c) R. Adhikary, J. Zimmermann, F. E. Romesberg, *Chem. Rev.* **2017**, *117*, 1927 – 1969.

[3] a) S. Hammes-Schiffer, S. J. Benkovic, *Annu. Rev. Biochem.* **2006**, *75*, 519 – 541; b) E. Z. Eisenmesser, O. Millet, W. Labeikovsky, D. M. Korzhnev, M. Wolf-Watz, D. A. Bosco, J. J. Skalicky, L. E. Kay, D. Kern, *Nature* **2005**, *438*, 117 – 121; c) S. J. Benkovic, S. Hammes-Schiffer, *Science* **2003**, *301*, 1196 – 1202; d) E. Z. Eisenmesser, D. A. Bosco, M. Akke, D. Kern, *Science* **2002**, *295*, 1520 – 1523; e) A. Hadzipasic, C. Wilson, V. Nguyen, N. Kern, C. Kim, W. Pitsawong, J. Villali, Y. J. Zheng, D. Kern, *Science* **2020**, *367*, 912 – 917.

[4] a) J. Ådén, M. Wolf-Watz, *J. Am. Chem. Soc.* **2007**, *129*, 14003 – 14012; b) A. J. Baldwin, L. E. Kay, *Nat. Chem. Biol.* **2009**, *5*, 808 – 814; c) J. N. Bandaria, S. Dutta, M. W. Nydegger, W. Rock, A. Kohen, C. M. Cheatum, *Proc. Natl. Acad. Sci. USA* **2010**, *107*, 17974 – 17979; d) Y. Choi, I. S. Moody, P. C. Sims, S. R. Hunt, B. L. Corso, D. E. Seitz, L. C. Blaszczak, P. G. Collins, G. A. Weiss, *J. Am. Chem. Soc.* **2012**, *134*, 2032 – 2035; e) V. I. Claessen, H. Engelkamp, P. C. M. Christianen, J. C. Maan, R. J. M. Nolte, K. Blank, A. E. Rowan, *Annu. Rev. Anal. Chem.* **2010**, *3*, 319 – 340; f) A. Sekhar, L. E. Kay, *Proc. Natl. Acad. Sci. USA* **2013**, *110*, 12867 – 12874; g) X. W. Zhuang, H. Kim, M. J. B. Pereira, H. P. Babcock, N. G. Walter, S. Chu, *Science* **2002**, *296*, 1473 – 1476.

[5] O. A. Sytina, D. J. Heyes, C. N. Hunter, M. T. Alexandre, I. H. M. van Stokkum, R. van Grondelle, M. L. Groot, *Nature* **2008**, *456*, 1001 – 1004.

[6] Y. Choi, I. S. Moody, P. C. Sims, S. R. Hunt, B. L. Corso, D. E. Seitz, L. C. Blaszczak, P. G. Collins, G. A. Weiss, *J. Am. Chem. Soc.* **2012**, *134*, 8286 – 8286.

[7] a) S. Ye, E. Zaitseva, G. Caltabiano, G. F. X. Schertler, T. P. Sakmar, X. Deupi, R. Vogel, *Nature* **2010**, *464*, 1386 – 1389; b) S. Ye, T. Huber, R. Vogel, T. P. Sakmar, *Nat. Chem. Biol.* **2009**, *5*, 397 – 399.

[8] K. C. Schultz, L. Supekova, Y. Ryu, J. Xie, R. Perera, P. G. Schultz, *J. Am. Chem. Soc.* **2006**, *128*, 13984 – 13985.

[9] C. Wilson, D. Kern, *Science* **2020**, *370*, 527 – 529.

[10] V. Nguyen, C. Wilson, M. Hoemberger, J. B. Stiller, R. V. Agafonov, S. Kutter, J. English, D. L. Theobald, D. Kern, *Science* **2017**, *355*, 289 – 293.

[11] C. Wilson, R. V. Agafonov, M. Hoemberger, S. Kutter, A. Zorba, J. Halpin, V. Buosi, R. Otten, D. Waterman, D. L. Theobald, D. Kern, *Science* **2015**, *347*, 882 – 886.

[12] a) L. Wang, P. G. Schultz, *Chem. Biol.* **2001**, *8*, 883 – 890; b) L. Wang, A. Brock, B. Herberich, P. G. Schultz, *Science* **2001**, *292*, 498 – 500.

[13] J. Zhang, L. Wang, J. Zhang, J. R. Zhu, X. Pan, Z. F. Cui, J. Y. Wang, W. H. Fang, Y. L. Li, *J. Phys. Chem. B* **2018**, *122*, 8122 – 8133.

[14] F. Perakis, L. De Marco, A. Shalit, F. J. Tang, Z. R. Kann, T. D. Kuhne, R. Torre, M. Bonn, Y. Nagata, *Chem. Rev.* **2016**, *116*, 7590 – 7607.

[15] a) K. Kwak, S. Park, I. J. Finkelstein, M. D. Fayer, *J. Chem. Phys.* **2007**, *127*, 124503; b) K. Kwak, D. E. Rosenfeld, M. D. Fayer, *J. Chem. Phys.* **2008**, *128*, 204505.

[16] K. Ramasesha, L. De Marco, A. Mandal, A. Tokmakoff, *Nat. Chem.* **2013**, *5*, 935 – 940.

[17] A. A. Bakulin, D. Cringus, P. A. Pieniazek, J. L. Skinner, T. L. C. Jansen, M. S. Pshenichnikov, *J. Phys. Chem. B* **2013**, *117*, 15545 – 15558.

[18] M. Peng, X. L. Chen, D. Zhang, X. J. Wang, N. Wang, P. Wang, J. D. Todd, Y. Z. Zhang, C. Y. Li, *Appl. Environ. Microbiol.* **2019**, *85*, e03127-18.

[19] L. B. Da Silva, J. E. Trebes, R. Balhorn, S. Mrowka, E. Anderson, D. T. Attwood, T. W. Barbee, J. Brase, M. Corzett, J. Gray, J. A. Koch, C. Lee, D. Kern, R. A. London, B. J. Macgowan, D. L. Matthews, G. Stone, *Science* **1992**, *258*, 269 – 271.

[20] a) C. L. Tsou, *Science* **1993**, *262*, 380 – 381; b) C. L. Zou, *Chin. Sci. Bull.* **1989**, *34*, 793 – 799; c) Z. Yuan, J. Zhao, Z. X. Wang, *Protein Eng.* **2003**, *16*, 109 – 114; d) Y. Wu, Z. X. Wang, *Biochim. Biophys. Acta Protein Struct. Mol. Enzymol.* **1998**, *1388*, 325 – 336; e) C. Wang, S. H. Chen, X. Wang, L. Wang, A. K. Wallis, R. B. Freedman, C. C. Wang, *J. Biol. Chem.* **2010**, *285*, 26788 – 26797; f) O. V. Stepanenko, I. M. Kuznetsova, K. K. Turoverov, C. J. Huang, C. C. Wang, *Biochemistry* **2004**, *43*, 5296 – 5303.

[21] H. T. Kratochvil, J. K. Carr, K. Matulef, A. W. Annen, H. Li, M. Maj, J. Ostmeyer, A. L. Serrano, H. Raghuraman, S. D. Moran, J. L. Skinner, E. Perozo, B. Roux, F. I. Valiyaveetil, M. T. Zanni, *Science* **2016**, *353*, 1040 – 1044.

Manuscript received: December 20, 2020
Revised manuscript received: February 10, 2021
Accepted manuscript online: February 28, 2021
Version of record online: April 7, 2021

